Numer. Math. (2013) 123:259–290
DOI 10.1007/s00211-012-0484-6

Numerische Mathematik

Explicit trace inequalities for isogeometric analysis and parametric hexahedral finite elements

John A. Evans · Thomas J. R. Hughes

Received: 27 May 2011 / Revised: 22 February 2012 / Published online: 10 July 2012

Abstract We derive new trace inequalities for NURBS-mapped domains. In addition to Sobolev-type inequalities, we derive discrete trace inequalities for use in NURBS-based isogeometric analysis. All dependencies on shape, size, polynomial degree, and the NURBS weighting function are precisely specified in our analysis, and explicit values are provided for all bounding constants appearing in our estimates. As hexahedral finite elements are special cases of NURBS, our results specialize to parametric hexahedral finite elements, and our analysis also generalizes to T-spline-based isogeometric analysis. We compare the bounding constants appearing in our explicit trace inequalities with numerically computed optimal bounding constants, and we discuss application of our results to a Laplace problem. We finish this paper with a brief exploration of so-called patch-wise trace inequalities for isogeometric analysis.

Mathematics Subject Classification 65N30 · 65N12

1 Introduction

Since its introduction in 2005 by Hughes et al. [24], isogeometric analysis has emerged as a powerful design-through-analysis technology. The underling concept behind isogeometric analysis is simple: utilize the same basis for finite element analysis (FEA) as is used to describe computer-aided design (CAD) geometry. The first instantiations of isogeometric analysis were based upon Non-Uniform Rational B-Splines (NURBS), and isogeometric analysis has since been extended to T-spline [4,16] and subdivision [13] discretizations. Isogeometric analysis has shown much promise in a wide variety of application areas such as structural analysis [15,17,28], fluid-structure interaction [5], and electromagnetism [12], and isogeometric analysis now has a firm theoretical

J. A. Evans (✉) · T. J. R. Hughes
Institute for Computational Engineering and Sciences, The University of Texas at Austin, Austin, USA
e-mail: evans@ices.utexas.edu

basis [6,11,21]. However, a number of research challenges remain. Among these challenges is the imposition of strong boundary conditions. Unlike Lagrange finite elements, NURBS, T-spline, and subdivision basis functions do not interpolate function values at nodal points. Imposition of strong boundary conditions is even less straightforward for fourth-order systems (such as those arising in Cahn–Hilliard phase-field models [22] and Kirchhoff plate and shell theories [25]) where strong boundary conditions involving normal derivatives naturally arise. Hence, special care must be taken in order to ensure an isogeometric discretization satisfies prescribed strong boundary conditions.

Recently, Nitsche's method [29] has been explored as a means of weakly enforcing strong boundary conditions in isogeometric analysis [8,18]. This procedure has been found to be especially powerful in isogeometric flow simulation where a close connection with so-called turbulent wall models has been discovered [7]. In Nitsche's method, a stabilization parameter appears which must be chosen large enough to ensure coercivity. Notably, the parameter should be chosen large enough such that a discrete trace inequality is satisfied. This requirement results in Nitsche parameters which necessarily depend locally on the shape of the element and the chosen discretization, but such dependencies have not yet been made explicit in the context of isogeometric analysis. In this paper, new trace inequalities for NURBS-based isogeometric analysis are derived where all dependencies on shape, size, polynomial degree, and the NURBS weighting function are precisely specified. Furthermore, explicit values are provided for bounding constants appearing in our estimates and, as such, these inequalities can be directly utilized in the design of Nitsche's stabilization parameter.

An outline of this paper is as follows. In Sect. 2, we briefly introduce requisite terminology and definitions. In Sect. 3, we derive a new Sobolev trace inequality for H^1 functions defined on NURBS-mapped domains. In Sect. 4, we derive discrete trace inequalities specifically for use in NURBS-based isogeometric analysis. In Sect. 5, we discuss the application of our discrete trace inequalities in the numerical solution of a Laplace problem, and in Sect. 6, we conduct a short exploration of so-called patch-wise trace inequalities for isogeometric analysis. Finally, in Sect. 7, we draw conclusions. Before proceeding, we would like to make a couple of remarks. First of all, the focus of this paper will be the three-dimensional setting. Similar results to those presented here hold in the two-dimensional setting, albeit with different constants. Second, while we only discuss NURBS-based isogeometric analysis, our results immediately apply to any isogeometric discretization technique based on rational functions. Notably, they apply to T-spline and parametric hexahedral finite element discretizations. Unfortunately, our results do not extend to subdivision discretizations as they are not rational.

2 Preliminaries

Throughout this paper, we make use of the classical Lebesgue spaces $L^q(D)$ endowed with norm $\|\cdot\|_{L^q(D)}$ where $1 \leq q \leq \infty$ and $D \subset \mathbb{R}^d$ is a generic open domain for integer $d \geq 1$. We will also utilize the Sobolev spaces $H^k(D)$ for k a positive integer, endowed with norm

$$\|u\|_{H^k(D)} := \left(\sum_{\alpha_1+\cdots+\alpha_d \le k} \left\| \frac{\partial^{\alpha_1}}{\partial x_1^{\alpha_1}} \cdots \frac{\partial^{\alpha_d}}{\partial^{\alpha_d} x_d} u \right\|^2_{L^2(D)} \right)^{1/2} \tag{1}$$

and semi-norm

$$|u|_{H^k(D)} := \left(\sum_{\alpha_1+\cdots+\alpha_d = k} \left\| \frac{\partial^{\alpha_1}}{\partial x_1^{\alpha_1}} \cdots \frac{\partial^{\alpha_d}}{\partial^{\alpha_d} x_d} u \right\|^2_{L^2(D)} \right)^{1/2}. \tag{2}$$

We denote by ∂D the boundary of an open domain $D \subset \mathbb{R}^d$, and we further denote by $\|\cdot\|_{L^2(\partial D)}$ the Lebesgue norm of order 2 on ∂D. We will occasionally employ the Sobolev spaces $W^{k,\infty}(D)$ for k a positive integer, and we endow these spaces with norm

$$\|u\|_{W^{k,\infty}} := \left(\sum_{\alpha_1+\cdots+\alpha_d \le k} \left\| \frac{\partial^{\alpha_1}}{\partial x_1^{\alpha_1}} \cdots \frac{\partial^{\alpha_d}}{\partial^{\alpha_d} x_d} u \right\|^2_{L^\infty(D)} \right)^{1/2} \tag{3}$$

and semi-norm

$$|u|_{W^{k,\infty}} := \left(\sum_{\alpha_1+\cdots+\alpha_d = k} \left\| \frac{\partial^{\alpha_1}}{\partial x_1^{\alpha_1}} \cdots \frac{\partial^{\alpha_d}}{\partial^{\alpha_d} x_d} u \right\|^2_{L^\infty(D)} \right)^{1/2}.$$

Note that these are not the classically defined norms and semi-norms for the $W^{k,\infty}$ spaces. For matrix-valued functions $\mathbf{M} : D \to \mathbb{R}^{m\times n}$, we define a spectral L^∞ operator norm

$$\begin{aligned} \|\mathbf{M}\|_{L^\infty(D),l} &:= \left\| \sup_{\mathbf{x}\in\mathbb{R}^m} \left(\frac{\sum_{j=1}^n \left(\sum_{i=1}^m M_{ij} x_i \right)^2}{\sum_{i=1}^m x_i^2} \right)^{1/2} \right\|_{L^\infty(D)} \\ &\equiv \|\sigma_{\max}(\mathbf{M})\|_{L^\infty(D)} \end{aligned} \tag{4}$$

where M_{ij} and x_i denote component-wise entries of $\mathbf{M}$ and $\mathbf{x}$ respectively and $\sigma_{\max}$ denotes maximum singular value. For third-order tensor-valued functions $\mathbf{T} : D \to \mathbb{R}^{m\times n\times o}$, we define an analogous L^∞ operator norm

$$\|\mathbf{T}\|_{L^\infty(D),l} := \left\| \sup_{\mathbf{x},\mathbf{y}\in\mathbb{R}^m} \left(\frac{\sum_{j=1}^n \left(\sum_{k=1}^o \sum_{i=1}^m T_{ijk} x_i y_k \right)^2}{\left(\sum_{i=1}^m x_i^2 \right) \left(\sum_{k=1}^o y_k^2 \right)} \right)^{1/2} \right\|_{L^\infty(D)} \tag{5}$$

where T_{ijk} denotes a component-wise entry of $\mathbf{T}$. The norms defined by (4) and (5) have been specially chosen as to simplify the analysis presented in this paper. The rest of this section will be devoted to a brief introduction of univariate and multivariate B-spline basis functions, NURBS basis functions, and the NURBS geometrical map $\mathbf{F}$.

A more complete introduction to NURBS and B-splines may be found in [30], and for an introductory text on NURBS-based isogeometric analysis, see [14].

2.1 Univariate B-splines

For two positive integers p and n, representing degree and dimensionality respectively, let us introduce the ordered knot vector

$$\Xi := \{0 = \xi_1, \xi_2, \ldots, \xi_{n+p+1} = 1\} \tag{6}$$

where

$$\xi_1 \leq \xi_2 \leq \cdots \xi_{n+p+1}.$$

Given Ξ and p, univariate B-spline basis functions are constructed recursively starting with piecewise constants ($p = 0$):

$$B_i^0(\xi) = \begin{cases} 1 & \text{if } \xi_i \leq \xi < \xi_{i+1} \\ 0 & \text{otherwise.} \end{cases} \tag{7}$$

For $p = 1, 2, 3, \ldots$, they are defined by

$$B_i^p(\xi) = \frac{\xi - \xi_i}{\xi_{i+p} - \xi_i} B_i^{p-1}(\xi) + \frac{\xi_{i+p+1} - \xi}{\xi_{i+p+1} - \xi_{i+1}} B_{i+1}^{p-1}(\xi). \tag{8}$$

When $\xi_{i+p} - \xi_i = 0$, $\frac{\xi - \xi_i}{\xi_{i+p} - \xi_i}$ is taken to be zero, and similarly, when $\xi_{i+p+1} - \xi_{i+1} = 0$, $\frac{\xi_{i+p+1} - \xi}{\xi_{i+p+1} - \xi_{i+1}}$ is taken to be zero. B-spline basis functions are piecewise polynomials of degree p, form a partition of unity, have local support, and are non-negative.

Let us now introduce the vector $\boldsymbol{\zeta} = \{\zeta_1, \ldots, \zeta_m\}$ of knots without repetitions and a corresponding vector $\{r_1, \ldots, r_m\}$ of knot multiplicities. That is, r_i is defined to be the multiplicity of the knot ζ_i in Ξ. By construction, $\sum_{i=1}^m r_i = n + p + 1$. We assume that $r_i \leq p + 1$. Let us further assume throughout that $r_1 = r_m = p + 1$, i.e, that Ξ is an *open* knot vector. At the point ζ_i, B-spline basis functions have $\alpha_j := p - r_j$ continuous derivatives. Therefore, $-1 \leq \alpha_j \leq p - 1$, and the maximum multiplicity allowed, $r_j = p + 1$, gives a discontinuity at ζ_j. By construction, $\alpha_1 = \alpha_m = -1$.

2.2 Multivariate tensor-product B-splines

The definition of multivariate B-splines follows easily through a tensor-product construction. Let us focus on the three-dimensional case. Notably, let us consider the unit cube $\widehat{\Omega} = (0, 1)^3 \subset \mathbb{R}^3$, which we refer to as the *patch*. Mimicking the one-dimensional case, given integers p_d and n_d for $d = 1, 2, 3$, let us introduce open knot vectors $\Xi_d = \{\xi_{1,d}, \ldots, \xi_{n_d+p_d+1,d}\}$ and the associated vectors $\boldsymbol{\zeta}_d = \{\zeta_{1,d}, \ldots, \zeta_{m_d,d}\}$, $\{r_{1,d}, \ldots, r_{m_d,d}\}$, and $\boldsymbol{\alpha}_d = \{\alpha_{1,d}, \ldots, \alpha_{m_d,d}\}$. There is a

parametric Cartesian mesh $\mathcal{Q}_h$ associated with these knot vectors partitioning the parametric domain $\widehat{\Omega}$ into rectangular parallelepipeds. Visually,

$$\mathcal{Q}_h = \{Q = \otimes_{d=1,2,3}(\zeta_{i_d,d}, \zeta_{i_d+1,d}),\ 1 \le i_d \le m_d - 1\}. \tag{9}$$

For each element $Q \in \mathcal{Q}_h$ we associate a parametric mesh size $h_Q = h_{Q,\max}$ where $h_{Q,\max}$ denotes the length of the largest edge of Q. Also, for each element, we define a shape regularity constant

$$\lambda_Q = \frac{h_Q}{h_{Q,\min}} \tag{10}$$

where $h_{Q,\min}$ denotes the length of the smallest edge of Q.

We associate with each knot vector Ξ_d $(d = 1, 2, 3)$ univariate B-spline basis functions $B_{i,d}^{p_d}$ of degree p_d for $i = 1, \ldots, n_d$. On the mesh $\mathcal{Q}_d$, we define the tensor-product B-spline basis functions as

$$B_{i,j,k}^{p_1,p_2,p_3} := B_{i,1}^{p_1} B_{j,2}^{p_2} B_{k,3}^{p_3}, \quad i = 1, \ldots, n_1,\ j = 1, \ldots, n_2,\ k = 1, \ldots, n_3. \tag{11}$$

Like their univariate counterparts, multivariate B-spline basis functions are piecewise polynomial, form a partition of unity, have local support, and are non-negative.

2.3 NURBS

Let us define a set of positive *weights* w_{ijk} for $1 \le i \le n_1$, $1 \le j \le n_2$, $1 \le k \le n_3$. The so-called NURBS basis functions are defined to be

$$R_{i,j,k}^{p_1 p_2 p_3} := \frac{w_{ijk} B_{i,j,k}^{p_1,p_2,p_3}}{w}, \quad i = 1, \ldots, n_1,\ j = 1, \ldots, n_2,\ k = 1, \ldots, n_3, \tag{12}$$

where $B_{ijk}^{p_1 p_2 p_3}$ are the B-spline basis functions defined in the previous subsection and w is the *weighting function* defined by

$$w = \sum_{i=1,j=1,k=1}^{n_1,n_2,n_3} w_{ijk} B_{i,j,k}^{p_1,p_2,p_3}. \tag{13}$$

Note that as multivariate B-spline basis functions form a partition of unity, the NURBS basis reduces to the B-spline basis when the weights are chosen to be unity. Also note that the NURBS basis functions are pointwise positive and form a partition of unity.

In NURBS-based isogeometric analysis, the physical domain is defined through a NURBS geometrical mapping

$$\mathbf{F} = \sum_{i=1,j=1,k=1}^{n_1,n_2,n_3} \mathbf{P}_{ijk} R_{ijk}^{p_1 p_2 p_3} \tag{14}$$

where $\mathbf{P}_{ijk} \in \mathbb{R}^3$ are the so-called *control points*. $\mathbf{F}$ is a parametrization of the physical domain Ω of interest, that is,

$$\mathbf{F} : (0, 1)^3 \to \Omega.$$

We assume throughout that $\mathbf{F}$ is invertible, with smooth inverse $\mathbf{F}^{-1}$, on each element $Q \in \mathcal{Q}_h$. NURBS are capable of representing all conic sections, such as circles and ellipses, and cylinders, spheres, tori, ellipsoids, are also exactly representable. In general, more than one patch must be utilized to represent a chosen geometry. In this situation, proper constraints should be enforced in order to ensure global continuity. For more on multi-patch geometries, see Chapter 2 of [14].

For each element Q in the parametric domain there is a corresponding *physical element* $K = \mathbf{F}(Q)$. We define the *physical mesh* to be

$$\mathcal{K}_h = \{K : K = \mathbf{F}(Q), \quad Q \in \mathcal{Q}_h\} = \mathbf{F}(\mathcal{Q}_h). \tag{15}$$

We define for each physical element $K \in \mathcal{K}_h$ a physical mesh size

$$h_K = \|\nabla \mathbf{F}\|_{L^\infty(Q),l} h_Q \tag{16}$$

where Q is the pre-image of K and $\nabla \mathbf{F}$ is the matrix of partial derivatives of the coordinate components of $\mathbf{F}$ (i.e., $(\nabla \mathbf{F})_{ij} = \frac{\partial F_i}{\partial \xi_j}$). We introduce the space $\mathcal{V}^h$ of NURBS on Ω (which is the *push-forward* of the space of NURBS on the patch $(0, 1)^3$)

$$\mathcal{V}^h := \text{span}\left\{ R_{i,j,k}^{p_1 p_2 p_3} \circ \mathbf{F}^{-1} \right\}_{i=1,j=1,k=1}^{n_1,n_2,n_3}. \tag{17}$$

In isogeometric analysis, the space $\mathcal{V}^h$ is utilized as the trial space in a Galerkin or Petrov–Galerkin method. Note that the functions in $\mathcal{V}^h$ are smooth on each physical element $K \in \mathcal{K}_h$, and the NURBS basis functions and weighting function are smooth on each parametric element $Q \in \mathcal{Q}_h$.

3 A Sobolev trace inequality for NURBS-mapped domains

Sobolev trace inequalities play an important role in the analysis of partial differential equations and their numerical solution. Generally speaking, these inequalities involve bounding the trace norm of a function by a constant multiplied by its interior norm. The precise value of this constant and its dependency on domain shape and size has been the focus of a collection of papers in the mathematics literature. Optimal Sobolev trace constants for the half-plane were derived by Beckner [10] and Escobar [20] based on earlier work of Lions [27]. Optimal constants for general domains were derived in [3], but the derived constants are specified in terms of an awkward and computationally prohibitive limiting procedure. Explicit, but not necessarily optimal, Sobolev trace constants for simplices and parallelepipeds were presented by Vesser and Verfürth in [32] for use in finite element a posteriori error estimation. In this section, we present

a new Sobolev trace inequality for NURBS-mapped domains. This trace inequality is completely explicit with respect to mesh size, parametric shape regularity, and local measures of the NURBS parametric mapping $\mathbf{F}$, and appropriate values are provided for the bounding constant appearing in our estimate. It should be noted that while the derived inequality is not necessarily sharp, special care is taken to ensure that the estimate is easily computable for utilization in numerical simulation.

3.1 General Lipschitz domains and the unit cube

We begin with the standard Sobolev trace theorem for general Lipschitz domains. Its proof may be found in [1], for example.

Theorem 3.1 *If $D \subset \mathbb{R}^3$ is a Lipschitz domain, then $H^1(D)$ is continuously embedded in $L^2(\partial D)$. That is, there exists a positive constant $C^*(D)$ such that, for all $f \in H^1(D)$,*

$$\|f\|^2_{L^2(\partial D)} \leq C^*(D)\|f\|^2_{H^1(D)}. \tag{18}$$

The constant $C^*(D)$ appearing above necessarily depends on the domain D, but the theorem does not explicitly specify such a dependence. In order to arrive at such a dependence for NURBS-mapped domains, let us first present the following corollary to Theorem 3.1.

Corollary 3.1 *There exists a positive constant C_u such that, for all $f \in H^1((0,1)^3)$,*

$$\|f\|^2_{L^2(\partial(0,1)^3)} \leq C_u\|f\|^2_{H^1((0,1)^3)}. \tag{19}$$

Note that the optimal constant appearing in (19) is precisely the maximizer of the Rayleigh quotient

$$\frac{\|f\|^2_{L^2(\partial(0,1)^3)}}{\|f\|^2_{H^1((0,1)^3)}} \tag{20}$$

where $f \in H^1((0,1)^3$. Hence, the optimal constant is equivalent to the largest eigenvalue λ_{max} of the generalized variational eigenproblem: find $f \in H^1((0,1)^3)$, $\lambda \in \mathbb{R}^+$ such that

$$(f,g)_{L^2(\partial(0,1)^3)} = \lambda(f,g)_{H^1((0,1)^3)}, \quad \forall g \in H^1((0,1)^3). \tag{21}$$

In order to arrive at the value of λ_{max}, we have numerically solved (21) using Galerkin's method in conjunction with a sequence of nested tri-cubic B-spline spaces. These computations reveal that the value of λ_{max}, up to ten significant figures, is

$$\lambda_{max} = 6.165748028\ldots \tag{22}$$

This value provides a sharp lower bound for the constant C_u appearing in Corollary 3.1. It is interesting that the Rayleigh quotient (20) is nearly maximized for constant f. This is also true for the unit line and the unit square.

3.2 The rectangular parallelepiped

We now derive a Sobolev trace inequality for the rectangular parallelepiped by utilizing a scaling argument. We note that the trace inequality is similar in nature to that of Corollary 4.5 of [32], but our method of proof and final result are ultimately different.

Lemma 3.1 *Let $D \subset \mathbb{R}^3$ denote a rectangular parallelepiped whose length, width, and height are h_1, h_2, and h_3 respectively. Then, for all $f \in H^1(D)$,*

$$\|f\|^2_{L^2(\partial D)} \leq \frac{C_u M}{V}\left(\|f\|^2_{L^2(D)} + N|f|^2_{H^1(D)}\right) \tag{23}$$

where C_u is a positive constant chosen large enough such that inequality (19) of Corollary 3.1 is satisfied and

$$\begin{aligned} M &:= \max\{h_1h_2, h_2h_3, h_1h_3\}, \\ N &:= \max\{h_1^2, h_2^2, h_3^2\}, \\ V &:= h_1h_2h_3 = \text{ the volume of } D. \end{aligned}$$

Proof Let $f \in H^1(D)$ denote an arbitrary function. We write

$$\|f\|^2_{L^2(\partial D)} = \int\limits_{\partial D} f^2 \, d\mathbf{s}.$$

We now expand the surface integral. We write

$$\int\limits_{\partial D} f^2 \, d\mathbf{s} = \int\limits_{D_{\text{top}}} + \int\limits_{D_{\text{bottom}}} + \int\limits_{D_{\text{left}}} + \int\limits_{D_{\text{right}}} + \int\limits_{D_{\text{front}}} + \int\limits_{D_{\text{back}}} f^2 \, d\mathbf{s} \tag{24}$$

where D_{top} denotes the top of the parallelepiped D and the other notation follows. Before proceeding, let $\mathbf{g} : [0,1]^3 \to \bar{D}$ denote the unique *face-preserving* affine function mapping the (closed) unit cube onto $\bar{D}$, the closure of the open domain D. That is, $\mathbf{g}$ maps the top face of the unit cube to the top face of D and so on. Let us now parameterize the surface integral using $\mathbf{g}$. We write:

$$\int\limits_{D_{\text{top}}} f^2 \, d\mathbf{s} = h_1h_2 \int\limits_0^1 \int\limits_0^1 f^2(\mathbf{g}(x_1, x_2, 1)) \, dx_1 \, dx_2$$

$$\int\limits_{D_{\text{bottom}}} f^2 \, d\mathbf{s} = h_1h_2 \int\limits_0^1 \int\limits_0^1 f^2(\mathbf{g}(x_1, x_2, 0)) \, dx_1 \, dx_2$$

$$\int\limits_{D_{\text{left}}} f^2 \, d\mathbf{s} = h_2h_3 \int\limits_0^1 \int\limits_0^1 f^2(\mathbf{g}(0, x_2, x_3)) \, dx_2 \, dx_3$$

$$\int_{D_{\text{right}}} f^2 \, d\mathbf{s} = h_2 h_3 \int_0^1 \int_0^1 f^2(\mathbf{g}(1, x_2, x_3)) \, dx_2 \, dx_3$$

$$\int_{D_{\text{front}}} f^2 \, d\mathbf{s} = h_1 h_3 \int_0^1 \int_0^1 f^2(\mathbf{g}(x_1, 0, x_3)) \, dx_1 \, dx_3$$

$$\int_{D_{\text{back}}} f^2 \, d\mathbf{s} = h_1 h_3 \int_0^1 \int_0^1 f^2(\mathbf{g}(x_1, 1, x_3)) \, dx_1 \, dx_3.$$

Noting the double integrals in the above expressions correspond to integration of the pullback $F = f \circ \mathbf{g}$ over the faces of the unit cube, we may insert the above six equations into (24) to obtain

$$\|f\|^2_{L^2(\partial D)} \leq M \int_{\partial(0,1)^3} F^2 \, d\mathbf{S} = M \|F\|^2_{L^2(\partial(0,1)^3)} \tag{25}$$

where

$$M = \max\{h_1 h_2, h_2 h_3, h_1 h_3\}.$$

By Corollary 3.1,

$$\|F\|^2_{L^2(\partial(0,1)^3)} \leq C_u \left(\|F\|^2_{L^2((0,1)^3)} + |F|^2_{H^1((0,1)^3)} \right) \tag{26}$$

where C_u is a positive constant chosen large enough such that (19) is satisfied. Applying a change of variables using the inverse of $\mathbf{g}$ to map back from the unit cube to D, we obtain

$$\|F\|^2_{L^2((0,1)^3)} = \frac{1}{V} \|f\|^2_{L^2(D)} \tag{27}$$

and

$$\begin{aligned} |F|^2_{H^1((0,1)^3)} &= \frac{h_1^2}{V} \|\partial_x f\|^2_{L^2(D)} + \frac{h_2^2}{V} \|\partial_y f\|^2_{L^2(D)} + \frac{h_3^2}{V} \|\partial_z f\|^2_{L^2(D)} \\ &\leq \frac{N}{V} |f|^2_{H^1(D)} \end{aligned} \tag{28}$$

where $V = h_1 h_2 h_3$ and $N = \max\{h_1^2, h_2^2, h_3^2\}$. The proof follows from combining (25)–(28). □

As a direct corollary of the above lemma, we have the following.

Corollary 3.2 *Let $D \subset \mathbb{R}^3$ denote a rectangular parallelepiped whose length, width, and height are h_1, h_2, and h_3 respectively. Let $h_D = \max\{h_1, h_2, h_3\}$ and let $\lambda_D \geq 1$ denote the local shape regularity constant*

$$\lambda_D = \frac{h_D}{\min\{h_1, h_2, h_3\}}. \tag{29}$$

Then, for all $f \in H^1(D)$,

$$\|f\|^2_{L^2(\partial D)} \leq C_u \lambda_D \left(h_D^{-1} \|f\|^2_{L^2(D)} + h_D |f|^2_{H^1(D)} \right) \tag{30}$$

where C_u *is a positive constant chosen large enough such that* (19) *is satisfied.*

3.3 NURBS-mapped domains

Armed with the theoretical results appearing in the previous subsection, we can finally prove a trace inequality for H^1 functions living on the physical mesh $\mathcal{K}_h$ which is explicit with respect to size and shape. The inequality is a simple consequence of pull-back operations between physical space and parametric space. Before proceeding, we would like to remark that the trace inequality provided here naturally extends to any rectangular parallelepiped mapped using a smooth mapping $\mathbf{F}$. Hence, it extends to iso- and subparametric hexahedral finite elements which are commonly used in practice.

Theorem 3.2 *Let* $K \in \mathcal{K}_h$ *and let* $Q = \mathbf{F}^{-1}(K)$. *Then, for all* $f \in H^1(K)$,

$$\|f\|^2_{L^2(\partial K)} \leq C_u \lambda_Q \lambda_K \left(h_K^{-1} \|f\|^2_{L^2(K)} + h_K |f|^2_{H^1(K)} \right) \tag{31}$$

where C_u *is a positive constant chosen large enough such that* (19) *is satisfied,* λ_Q *is the local shape regularity constant of* Q,

$$\lambda_K = \|\text{cof}(\nabla \mathbf{F})\|_{L^\infty(Q),I} \|\det(\nabla \mathbf{F}^{-1})\|_{L^\infty(K)} \|\nabla \mathbf{F}\|_{L^\infty(Q),I}, \tag{32}$$

$\text{cof}(\nabla \mathbf{F})$ *is the cofactor matrix of* $\nabla \mathbf{F}$, *and* $\det(\nabla \mathbf{F}^{-1})$ *is the determinant of* $\nabla \mathbf{F}^{-1}$.

Proof Let $f \in H^1(K)$. We write

$$\|f\|^2_{L^2(\partial K)} = \int_{\partial K} f^2 \, d\mathbf{s}.$$

Let us separate the surface integral into a collection of integrals over "faces". That is, let us write

$$\int_{\partial K} f^2 \, d\mathbf{s} = \int_{K_{\text{top}}} + \int_{K_{\text{bottom}}} + \int_{K_{\text{left}}} + \int_{K_{\text{right}}} + \int_{K_{\text{front}}} + \int_{K_{\text{back}}} f^2 \, d\mathbf{s}$$

where we have defined, for example, $K_{\text{top}} = \mathbf{F}(Q_{\text{top}})$ where Q_{top} is the top face of the rectangular parallelepiped Q. Note that, by construction,

$$Q = \otimes_{d=1,2,3} (\zeta_{i_d,d}, \zeta_{i_d+1,d})$$

for some $1 \leq i_d \leq m_d - 1$ where $d = 1, 2, 3$. We can then write the surface integral for the top face of K as

$$\int_{K_{\text{top}}} f^2 \, d\mathbf{s} = \int_{\zeta_{i_2,2}}^{\zeta_{i_2+1,2}} \int_{\zeta_{i_1,1}}^{\zeta_{i_1+1,1}} f^2(\mathbf{F}(\xi_1, \xi_2, \zeta_{i_3+1,3})) J(\xi_1, \xi_2, \zeta_{i_3+1,3}) \, d\xi_1 \, d\xi_2$$

where

$$J(\xi_1, \xi_2, \xi_3) = \left| \frac{\partial \mathbf{F}(\xi_1, \xi_2, \xi_3)}{\partial \xi_1} \times \frac{\partial \mathbf{F}(\xi_1, \xi_2, \xi_3)}{\partial \xi_2} \right|.$$

As $D\mathbf{F}$ is smooth on Q, we have that

$$J(\xi_1, \xi_2, \zeta_{i_3+1,3}) \leq \|\text{cof}(\nabla \mathbf{F})\|_{L^\infty(Q),l}$$

for all $\xi_1 \in (\zeta_{i_1,1}, \zeta_{i_1+1,1})$ and $\xi_2 \in (\zeta_{i_2,2}, \zeta_{i_2+1,2})$ where $\text{cof}(\nabla \mathbf{F})$ is the cofactor matrix of $\nabla \mathbf{F}$. Thus,

$$\int_{K_{\text{top}}} f^2 \, d\mathbf{s} \leq \|\text{cof}(\nabla \mathbf{F})\|_{L^\infty(Q),l} \int_{\zeta_{i_2,2}}^{\zeta_{i_2+1,2}} \int_{\zeta_{i_1,1}}^{\zeta_{i_1+1,1}} f^2(\mathbf{F}(\xi_1, \xi_2, \zeta_{i_3+1,1})) \, d\xi_1 \, d\xi_2.$$

Note that the remaining double integral in the above expression is precisely the surface integral for the square of the pullback $f \circ \mathbf{F}$ over the top face of Q. If we repeat the above process for the other faces of K and sum all of the resulting expressions, we obtain the inequality

$$\|f\|^2_{L^2(\partial K)} \leq \|\text{cof}(\nabla \mathbf{F})\|_{L^\infty(Q),l} \|f \circ \mathbf{F}\|^2_{L^2(\partial Q)}. \tag{33}$$

Now let us apply the trace inequality given by Corollary 3.2. This gives

$$\|f \circ \mathbf{F}\|^2_{L^2(\partial Q)} \leq C_u \lambda_Q \left(h_Q^{-1} \|f \circ \mathbf{F}\|^2_{L^2(Q)} + h_Q |f \circ \mathbf{F}|^2_{H^1(Q)} \right) \tag{34}$$

where λ_Q is the shape regularity constant for element Q and C_u is a positive constant chosen large enough such that (19) is satisfied. An application of change of variables, Hölder's inequality (see Appendix 8), and the definition of the spectral norm for matrices results in

$$\|f \circ \mathbf{F}\|^2_{L^2(Q)} \leq \|\det(\nabla \mathbf{F}^{-1})\|_{L^\infty(K)} \|f\|^2_{L^2(K)} \tag{35}$$

$$|f \circ \mathbf{F}|^2_{H^1(Q)} \leq \|\det(\nabla \mathbf{F}^{-1})\|_{L^\infty(K)} \|\nabla \mathbf{F}\|^2_{L^\infty(Q),l} |f|^2_{H^1(K)} \tag{36}$$

where $\det(\nabla \mathbf{F}^{-1})$ is the determinant of $\nabla \mathbf{F}^{-1}$. Combining (33)–(36) gives

$$\|f\|^2_{L^2(\partial K)} \leq C_u \lambda_Q \|\text{cof}(\nabla \mathbf{F})\|_{L^\infty(Q),l} \left(C_1 h_Q^{-1} \|f\|^2_{L^2(K)} + C_2 h_Q |f|^2_{H^1(K)} \right). \tag{37}$$

where

$$C_1 = \|\det(\nabla \mathbf{F}^{-1})\|_{L^\infty(K)}$$

and

$$C_2 = \|\det(\nabla \mathbf{F}^{-1})\|_{L^\infty(K)} \|\nabla \mathbf{F}\|^2_{L^\infty(Q),l},$$

and combining (37) with the definition

$$h_K = \|\nabla \mathbf{F}\|_{L^\infty(Q),l} h_Q$$

finally gives the desired result. □

It should be noted that the constant $\lambda_Q \lambda_K$ appearing in the above theorem is a dimensionless measure of physical shape regularity. This can be seen by observing that $\|\text{cof}(\nabla \mathbf{F})\|_{L^\infty(Q),l}$ is a measure of how planes in Q are expanded under $\mathbf{F}$, $\|\nabla \mathbf{F}\|_{L^\infty(Q),l}$ is a measure of how lines in Q are lengthened under $\mathbf{F}$, and $\|\det(\nabla \mathbf{F}^{-1})\|_{L^\infty(K)}$ is an inverse measure of how volumes in Q are expanded under $\mathbf{F}$. The multiplication of these three quantities by the local parametric shape regularity gives the physical shape regularity. Also, recall that we have a sharp lower bound estimate for the bounding constant C_u appearing in (31). Hence, Theorem 3.2 gives a practically computable trace constant. Finally, note that if $\mathbf{F}$ is taken to be the identity mapping, then $\lambda_K = 1$. If we had utilized alternative matrix norms in our analysis such as the Frobenius norm, we would have obtained $\lambda_K > 1$.

Remark Technically, $\mathbf{F}$ is a mapping of the open set $(0, 1)^3$ and consequently *not* a vector field. That being said, $\nabla \mathbf{F}$ is a common abuse of notation meaning $D\mathbf{F}$ in the sense of calculus on manifolds [26].

4 Discrete trace inequalities for isogeometric analysis

Discrete trace inequalities belong to a special class of inverse-type inequalities which are posed over discrete function spaces. Discrete trace inequalities play an important role in the selection of stabilization parameters for Nitsche's method [29], and they also play a critical role in the design of symmetric interior penalty methods [2,34]. Heretofore, the derivation of explicit discrete trace inequalities has been largely limited to simplex elements [19,31,33]. In this section, we derive new explicit discrete trace inequalities for use in NURBS-based isogeometric analysis where all dependencies on shape, size, polynomial degree, and the NURBS weighting function are precisely specified. As in the previous section, special care is taken to ensure that the derived estimates are easily computable for use in numerical simulation.

4.1 Discrete trace inequalities for tensor-product polynomials on rectangular parallelepipeds

We begin this section by deriving discrete trace inequalities for tensor-product polynomials on rectangular parallelepipeds. In order to conduct such a derivation, we will need the following lemma.

Lemma 4.1 *Let $\mathcal{P}^h = \mathcal{P}^{p_1,p_2,p_3}$ denote the space of tensor-product polynomials of degree (p_1, p_2, p_3) defined on $\mathbb{R}^3$. Then, for all $p^h \in \mathcal{P}^h$,*

$$\|p^h\|^2_{L^2(\partial(0,1)^3)} \leq C_{inv}(p_1, p_2, p_3)\|p^h\|^2_{L^2((0,1)^3)} \tag{38}$$

where

$$C_{inv}(p_1, p_2, p_3) = 2((p_1+1)^2 + (p_2+1)^2 + (p_3+1)^2). \tag{39}$$

Proof Let $p^h \in \mathcal{P}^h$. Since p^h is a tensor-product polynomial of degree (p_1, p_2, p_3), we can write

$$p^h(x_1, x_2, x_3) = \sum_{i=0,j=0,k=0}^{p_1,p_2,p_3} C_{ijk}N_i(x_1)N_j(x_2)N_k(x_3)$$

where N_l is the normalized shifted Legendre polynomial of degree l such that

$$\int_0^1 N_i(x)N_j(x)\,dx = \begin{cases} 1 & \text{if } i = j \\ 0 & \text{else} \end{cases}$$

and $C_{ijk} \in \mathbb{R}$ are appropriately chosen constants. By construction,

$$\|p^h\|^2_{L^2((0,1)^3)} = \sum_{i=0,j=0,k=0}^{p_1,p_2,p_3} C^2_{ijk}.$$

Now let us decompose

$$\begin{aligned}
\|p^h\|^2_{L^2(\partial(0,1)^3)} = &\int_0^1\int_0^1 \left(\sum_{i=0,j=0,k=0}^{p_1,p_2,p_3} C_{ijk}N_i(0)N_j(x_2)N_k(x_3)\right)^2 dx_2\,dx_3 \\
&+ \int_0^1\int_0^1 \left(\sum_{i=0,j=0,k=0}^{p_1,p_2,p_3} C_{ijk}N_i(1)N_j(x_2)N_k(x_3)\right)^2 dx_2\,dx_3 \\
&+ \int_0^1\int_0^1 \left(\sum_{i=0,j=0,k=0}^{p_1,p_2,p_3} C_{ijk}N_i(x_1)N_j(0)N_k(x_3)\right)^2 dx_1\,dx_3
\end{aligned}$$

$$+\int_0^1\int_0^1\left(\sum_{i=0,j=0,k=0}^{p_1,p_2,p_3} C_{ijk}N_i(x_1)N_j(1)N_k(x_3)\right)^2 dx_1\,dx_3$$
$$+\int_0^1\int_0^1\left(\sum_{i=0,j=0,k=0}^{p_1,p_2,p_3} C_{ijk}N_i(x_1)N_j(x_2)N_k(0)\right)^2 dx_1\,dx_2$$
$$+\int_0^1\int_0^1\left(\sum_{i=0,j=0,k=0}^{p_1,p_2,p_3} C_{ijk}N_i(x_1)N_j(x_2)N_k(1)\right)^2 dx_1\,dx_2. \tag{40}$$

If we take advantage of the orthonormality properties of our shifted Legendre polynomials, we can write

$$\int_0^1\int_0^1\left(\sum_{i=0,j=0,k=0}^{p_1,p_2,p_3} C_{ijk}N_i(0)N_j(x_2)N_k(x_3)\right)^2 dx_2\,dx_3$$
$$=\sum_{j=0,k=0}^{p_2,p_3}\left(\sum_{i=0}^{p_1} C_{ijk}N_i(0)\right)^2.$$

Now we employ Theorem 3.1 of [33], which states that

$$|f(0)| \le (p+1)\|f\|_{L^2(0,1)} \tag{41}$$

for every polynomial f of degree p. Since $\sum_{i=0}^{p_1} C_{ijk}N_i$ is a polynomial of degree p_1 for every j, k, we can utilize Theorem 3.1 of [33] and orthonormality to obtain

$$\sum_{j=0,k=0}^{p_2,p_3}\left(\sum_{i=0}^{p_1} C_{ijk}N_i(0)\right)^2 \le (p_1+1)^2\sum_{j=0,k=0}^{p_2,p_3}\int_0^1\sum_{i=0}^{p_1}(C_{ijk}N_i(x_1))^2\,dx_1$$
$$=(p_1+1)^2\sum_{i=0,j=0,k=0}^{p_1,p_2,p_3} C_{ijk}^2$$
$$=(p_1+1)^2\|p^h\|^2_{L^2((0,1)^3)}$$

By repeating this process to bound the other five terms appearing in (40), we obtain the desired expression. □

We would like to mention that while the constant C_{inv} appearing in the above trace inequality is not necessarily sharp, it is completely explicit with respect to polynomial degree. We believe this to be a significant advantage of our derived estimate. Alternatively, one can solve the generalized eigenvalue problem inferred by (38) to arrive at an optimal bounding constant (see, for example, [23]). In Table 1, we have compared

Table 1 Explicit values for the bounding constant in (38) versus the optimal value

Polynomial degree (p_1, p_2, p_3)	Explicit bounding constant	Optimal bounding constant
(0, 0, 0)	6	6
(1, 1, 1)	24	18
(2, 2, 2)	54	36
(3, 3, 3)	96	60
(4, 4, 4)	150	90
(5, 5, 5)	216	126
(6, 6, 6)	294	168
(7, 7, 7)	384	216
(8, 8, 8)	486	270
(1, 1, 2)	34	24
(1, 1, 3)	48	32
(1, 2, 2)	44	24
(1, 2, 3)	58	32
(2, 2, 3)	68	44
(2, 3, 3)	82	45.797958...

our explicit bounding constant with the optimal bounding constant for a wide range of polynomial degrees. From the table, we observe that our explicit bounding constant is of the same order of magnitude as the optimal bounding constant and scales optimally with polynomial degree.

Lemma 4.2 *Let $D \subset \mathbb{R}^3$ denote a rectangular parallelepiped whose length, width, and height are h_1, h_2, and h_3 respectively, and define $\mathcal{P}^h = \mathcal{P}^{p_1,p_2,p_3}$ to be the space of tensor-product polynomials of degree (p_1, p_2, p_3). Let $h_D = \max\{h_1, h_2, h_3\}$ and let $\lambda_D \geq 1$ denote the local shape regularity constant*

$$\lambda_D = \frac{h_D}{\min\{h_1, h_2, h_3\}}. \tag{42}$$

Then, for all $p^h \in \mathcal{P}^h$,

$$\|p^h\|^2_{L^2(\partial D)} \leq C_{inv}\lambda_D h_D^{-1} \|p^h\|^2_{L^2(D)}. \tag{43}$$

where $C_{inv} = C_{inv}(p_1, p_2, p_3)$ is the positive constant defined by Eq. (39).

Proof Let $p^h \in \mathcal{P}^h$. We utilize the same scaling argument as in the proof of Lemma 3.1. Notably, letting $\mathbf{g} : [0,1]^3 \to \bar{D}$ denote the unique face-preserving affine function mapping the closed unit cube onto $\bar{D}$ (the closure of D) and defining $P^h = p^h \circ \mathbf{g}$, we can write

$$\|p^h\|^2_{L^2(\partial D)} \leq M \int_{\partial(0,1)^3} (P^h)^2 \, d\mathbf{S} = M \|P^h\|^2_{L^2(\partial(0,1)^3)}$$

Table 2 Explicit values for the bounding constant in (43) versus the optimal value

Polynomial degree (p_1, p_2, p_3) is chosen to be (3, 3, 3) and the length, width, and height of the parallelepiped are chosen to be $h_1 = 1/\lambda_D$, $h_2 = 1/\lambda_D$, and $h_3 = 1$

Shape regularity λ_D	Explicit bounding constant	Optimal bounding constant
1	96	60
2	192	100
4	384	180
8	768	340
16	1,536	660
32	3,072	1,300

where

$$M = \max\{h_1 h_2, h_2 h_3, h_1 h_3\}.$$

By Lemma 4.1,

$$\|P^h\|^2_{L^2(\partial(0,1)^3)} \leq C_{inv} \|P^h\|^2_{L^2((0,1)^3)}$$

where $C_{inv} = C_{inv}(p_1, p_2, p_3)$ is the positive constant defined by Eq. (39). A simple change of variables formula gives

$$\|P^h\|^2_{L^2((0,1)^3)} = \frac{1}{h_1 h_2 h_3} \|p^h\|^2_{L^2(D)}$$

and the desired result follows by concatenating all of the above equalities and inequalities. □

In Table 2, we have compared our explicit bounding constant with the optimal bounding constant for a wide range of shape regularity factors and for polynomial degree $(p_1, p_2, p_3) = (3, 3, 3)$. From the table, we observe our explicit bounding constant is of the same order of magnitude as the optimal bounding constant and scales optimally with shape regularity.

4.2 Discrete trace inequalities for NURBS-based isogeometric analysis with locally constant weighting function

In this subsection, we derive discrete trace inequalities for isogeometric functions defined on NURBS-mapped domains where the weighting function is locally constant. This setting arises frequently in practice such as when polynomial-based B-splines are employed instead of more general NURBS discretizations. Furthermore, this setting makes for a much more straight-forward analysis which will be expanded upon later. We begin with the following lemma, which bounds the element trace of an isogeometric function by its interior L^2 norm.

Lemma 4.3 *Let $K \in \mathcal{K}_h$ and $Q = \mathbf{F}^{-1}(K)$. Suppose that the NURBS weighting function w, defined by (13), is chosen such that it is constant over Q. Then, for all*

$u^h \in \mathcal{V}^h$, defined in (17),

$$\|u^h\|^2_{L^2(\partial K)} \leq C_{inv}\lambda_Q\lambda_K h_K^{-1}\|u^h\|^2_{L^2(K)} \tag{44}$$

where $C_{inv} = C_{inv}(p_1, p_2, p_3)$ is the positive constant defined by (39), λ_Q is the local shape regularity constant of Q, and λ_K is the shape regularity constant defined by (32).

Proof Let $u^h \in \mathcal{V}^h$. To begin, we employ a change of variables from physical space to parametric space and utilize a similar argument to that used in the proof of Theorem 3.2 to arrive at

$$\|u^h\|^2_{L^2(\partial K)} \leq \|\mathrm{cof}(\nabla \mathbf{F})\|_{L^\infty(Q),l}\|u^h \circ \mathbf{F}\|^2_{L^2(\partial Q)}.$$

Noting that by supposition $u^h \circ \mathbf{F}$ is a polynomial over Q, we invoke Lemma 4.2 to obtain the expression

$$\|u^h\|^2_{L^2(\partial K)} \leq C_{inv}\lambda_Q h_Q^{-1}\|\mathrm{cof}(\nabla \mathbf{F})\|_{L^\infty(Q),l}\|u^h \circ \mathbf{F}\|^2_{L^2(Q)}$$

where $C_{inv} = C_{inv}(p_1, p_2, p_3)$ is the positive constant defined by (39), λ_Q is the local shape regularity constant of Q, and h_Q is the length of the largest side of Q. Finally, mapping back to physical space, we have

$$\|u^h\|^2_{L^2(\partial K)} \leq C_{inv}\lambda_Q h_Q^{-1}\|\mathrm{cof}(\nabla \mathbf{F})\|_{L^\infty(Q),l}\|\det(\nabla \mathbf{F}^{-1})\|_{L^\infty(K)}\|u^h\|^2_{L^2(K)}.$$

The lemma follows by recalling the definitions of λ_K and h_K. □

Before proceeding, we would like to note the similarity in form between the inequalities appearing in Theorem 3.2 and Lemma 4.3. Notably, both contain a bounding constant, a shape regularity factor, and mesh scaling terms. Furthermore, the bounding constants appearing in both inequalities are explicitly given.

We now present an inequality which bounds the element boundary normal derivative of an isogeometric function by its interior H^1 semi-norm. Such an inequality plays an important role in the design and analysis of Nitsche's method as applied to second-order elliptic problems.

Lemma 4.4 *Let $K \in \mathcal{K}_h$ and $Q = \mathbf{F}^{-1}(K)$. Suppose that the NURBS weighting function w is chosen such that is constant over Q. Then, for all $u^h \in \mathcal{V}^h$,*

$$\|\nabla u^h \cdot \mathbf{n}\|^2_{L^2(\partial K)} \leq C_B C_{inv}\lambda_Q\lambda_K h_K^{-1}|u^h|^2_{H^1(K)} \tag{45}$$

where $\mathbf{n}$ is the unit outward-facing normal, $C_{inv} = C_{inv}(p_1, p_2, p_3)$ is the positive constant defined by (39), λ_Q is the local shape regularity constant of Q, λ_K is the shape regularity constant defined by (32),

$$C_B = (1 + \sqrt{3}\|\nabla \mathbf{F}\|_{L^\infty(Q),l}\|\nabla^2 \mathbf{F}^{-1}\|_{L^\infty(K),l}h_K)^2, \tag{46}$$

and $\nabla^2 \mathbf{F}^{-1}$ *is the third-order tensor-valued function*

$$(\nabla^2 \mathbf{F}^{-1})_{ijk} = \frac{\partial^2 F_i^{-1}}{\partial x_j \partial x_k}. \tag{47}$$

Proof Let $u^h \in \mathcal{V}^h$. To begin, we employ a change of variables from physical space to parametric space:

$$\begin{aligned} \|\nabla u^h \cdot \mathbf{n}\|^2_{L^2(\partial K)} &\leq \int_{\partial K} |\nabla u^h|^2 \, d\mathbf{s} \\ &\leq \|\mathrm{cof}(\nabla \mathbf{F})\|_{L^\infty(Q),l} \int_{\partial Q} |(\nabla \mathbf{F}^{-1} \circ \mathbf{F})^T \nabla (u^h \circ \mathbf{F})|^2 \, d\mathbf{t}. \end{aligned} \tag{48}$$

Note that we cannot immediately utilize Lemma 4.2 as the components of the vector

$$(\nabla \mathbf{F}^{-1} \circ \mathbf{F})^T \nabla (u^h \circ \mathbf{F})$$

are not necessarily polynomial. For this reason, we employ the decomposition

$$\nabla \mathbf{F}^{-1} \circ \mathbf{F} = \mathbf{D} = \overline{\mathbf{D}} + \mathbf{D}' \tag{49}$$

where

$$\overline{\mathbf{D}} = \mathbf{D}(\boldsymbol{\xi}_c)$$

and $\boldsymbol{\xi}_c$ is the centroid of Q. Inserting the decomposition (49) into (48), applying the Cauchy–Schwarz inequality, invoking the definition of the spectral norm for matrices, and then applying Hölder's inequality on the resulting term involving $\mathbf{D}'$, we obtain

$$\begin{aligned} &\|\nabla u^h \cdot \mathbf{n}\|^2_{L^2(\partial K)} \\ &\quad \leq C_{cof} \left(\left(\int_{\partial Q} |\overline{\mathbf{D}}^T \nabla \left(u^h \circ \mathbf{F} \right)|^2 \, d\mathbf{t} \right)^{1/2} + \|\mathbf{D}'\|_{L^\infty(Q),l} |u^h \circ \mathbf{F}|_{H^1(\partial Q)} \right)^2 \end{aligned}$$

where

$$C_{cof} = \|\mathrm{cof}(\nabla \mathbf{F})\|_{L^\infty(Q),l}$$

We can now finally invoke Lemma 4.2, giving us the result

$$\begin{aligned}&\|\nabla u^h \cdot \mathbf{n}\|^2_{L^2(\partial K)}\\ &\leq C_{trace}C_{cof}\left(\left(\int_Q |\overline{\mathbf{D}}^T \nabla \left(u^h \circ \mathbf{F}\right)|^2 d\boldsymbol{\xi}\right)^{1/2} + \|\mathbf{D}'\|_{L^\infty(Q),l}|u^h \circ \mathbf{F}|_{H^1(Q)}\right)^2\end{aligned} \tag{50}$$

where

$$C_{trace} = C_{inv}(p_1, p_2, p_3)\lambda_Q h_Q^{-1}.$$

Again invoking the decomposition (49), the Cauchy–Schwarz inequality, the definition of the spectral norm for matrices, and Hölder's inequality, we obtain

$$\begin{aligned}\left(\int_Q |\overline{\mathbf{D}}^T \nabla \left(u^h \circ \mathbf{F}\right)|^2 d\boldsymbol{\xi}\right)^{1/2} &\leq \left(\int_Q |\mathbf{D}^T \nabla \left(u^h \circ \mathbf{F}\right)|^2 d\boldsymbol{\xi}\right)^{1/2}\\ &\quad + \|\mathbf{D}'\|_{L^\infty(Q),l}|u^h \circ \mathbf{F}|_{H^1(Q)}.\end{aligned} \tag{51}$$

By concatenating (50) and (51), we arrive at

$$\begin{aligned}\|\nabla u^h \cdot \mathbf{n}\|^2_{L^2(\partial K)} \leq C_{trace}C_{cof}&\left(\left(\int_Q |\mathbf{D}^T \nabla \left(u^h \circ \mathbf{F}\right)|^2 \, d\boldsymbol{\xi}\right)^{1/2}\right.\\ &\left. + 2\|\mathbf{D}'\|_{L^\infty(Q),l}|u^h \circ \mathbf{F}|_{H^1(\partial Q)}\right)^2\end{aligned} \tag{52}$$

Note that a change of variables gives

$$\left(\int_Q |\mathbf{D}^T \nabla \left(u^h \circ \mathbf{F}\right)|^2 \, d\boldsymbol{\xi}\right)^{1/2} \leq \|\det(\nabla \mathbf{F}^{-1})\|^{1/2}_{L^\infty(K)}|u^h|_{H^1(K)} \tag{53}$$

and (36) gives

$$|u^h \circ \mathbf{F}|_{H^1(Q)} \leq \|\det(\nabla \mathbf{F}^{-1})\|^{1/2}_{L^\infty(K)}\|\nabla \mathbf{F}\|_{L^\infty(Q),l}|u^h|_{H^1(K)}. \tag{54}$$

To complete the proof, we recognize that, by Taylor's theorem,

$$\begin{aligned}\|\mathbf{D}'\|_{L^\infty(Q),l} &= \|\mathbf{D} - \overline{\mathbf{D}}\|_{L^\infty(Q),l} \\ &\leq \frac{\sqrt{3}}{2} h_Q \|\nabla \mathbf{D}\|_{L^\infty(Q),l} \\ &\leq \frac{\sqrt{3}}{2} h_Q \|\nabla \mathbf{F}\|_{L^\infty(Q),l} \|\nabla^2 \mathbf{F}^{-1}\|_{L^\infty(K),l} \\ &\leq \frac{\sqrt{3}}{2} h_K \|\nabla^2 \mathbf{F}^{-1}\|_{L^\infty(K),l} \end{aligned} \tag{55}$$

Combining (52)–(55) with the definitions of the physical mesh size h_K and the physical shape regularity constant λ_K results in the desired final expression. □

Note that if we take the physical mesh size $h_K \to 0$ and keep the parametric mapping $\mathbf{F}$ fixed, the constant C_B appearing in the above theorem will tend to 1.0. Hence, we recover a similar inequality to that appearing in Lemma 4.3. This suggests that we may be able to ignore in practice higher-order terms due to the nonlinear geometrical mapping.

By employing a similar method of proof to that of Lemma 4.4, we can obtain discrete trace inequalities for higher-order boundary derivatives. For example, we can show that for a given element $K \in \mathcal{K}_h$ with $Q = \mathbf{F}^{-1}(K)$,

$$\|\Delta u^h\|^2_{L^2(\partial K)} \leq C_B C_{inv} \lambda_Q \lambda_K h_K^{-1} \|u^h\|^2_{H^2(K)}$$

for every $u^h \in \mathcal{V}^h$ where

$$C_B = 1 + O(h_K).$$

Such an inequality plays an important role in the design and analysis of Nitsche's method as applied to fourth-order elliptic problems. It can be shown that the explicit form for the constant C_B appearing in the above inequality is substantially more complicated than the corresponding constant appearing in Lemma 4.4, and this trend only worsens with further differentiation. Moreover, note that a full H^2 norm appears rather than just the H^2 semi-norm. However, in practice, it may be sufficient to replace C_B with 1.0.

Note that when the parametric mapping $\mathbf{F}$ exhibits a singularity, the constants appearing in the discrete trace inequalities given by Lemmata 4.3 and 4.4 blow up. This blow up is expected. Indeed, in the presence of a parametric singularity, the functions $u^h \in \mathcal{V}^h$ no longer lie in $H^1(K)$. This lack of regularity can be remedied by coalescing degrees of freedom (see Section 4.2 and Appendix 10.A of [14] for examples). This coalescence is analogous to the degenerated element concept. An alternate analysis must be conducted in order to derive trace inequalities which do not blow up for these configurations. Such an analysis is beyond the scope of the current paper.

4.3 Discrete trace inequalities for NURBS-based isogeometric analysis with general weighting function

Finally, we are ready to derive discrete trace inequalities for NURBS-based isogeometric analysis with general weighting function. We begin with the following theorem, which is a straight-forward extension of Lemma 4.3 to the general setting.

Theorem 4.1 *Let $K \in \mathcal{K}_h$ and $Q = \mathbf{F}^{-1}(K)$. Then, for all $u^h \in \mathcal{V}^h$,*

$$\|u^h\|^2_{L^2(\partial K)} \leq C_w C_{inv} \lambda_Q \lambda_K h_K^{-1} \|u^h\|^2_{L^2(K)} \tag{56}$$

where $C_{inv} = C_{inv}(p_1, p_2, p_3)$ is the positive constant defined by (39), λ_Q is the local shape regularity constant of Q, λ_K is the shape regularity constant defined by (32), and

$$C_w = \left\| \frac{1}{w} \right\|^2_{L^\infty(Q)} \|w\|^2_{L^\infty(Q)}. \tag{57}$$

Proof The proof proceeds in a similar manner to that of Lemma 4.3. Let $u^h \in \mathcal{V}^h$. We employ a change of variables from physical space to parametric space to arrive at

$$\|u^h\|^2_{L^2(\partial K)} \leq \|\mathrm{cof}(\nabla \mathbf{F})\|_{L^\infty(Q),l} \|u^h \circ \mathbf{F}\|^2_{L^2(\partial Q)}.$$

Now, we utilize Hölder's inequality to obtain

$$\|u^h\|^2_{L^2(\partial K)} \leq \|\mathrm{cof}(\nabla \mathbf{F})\|_{L^\infty(Q),l} \left\| \frac{1}{w} \right\|^2_{L^\infty(Q)} \|w(u^h \circ \mathbf{F})\|^2_{L^2(\partial Q)}.$$

Noting that $w(u^h \circ \mathbf{F})$ is a polynomial over Q, we invoke Lemma 4.2 to obtain the expression

$$\|u^h\|^2_{L^2(\partial K)} \leq C_{inv} \lambda_Q h_Q^{-1} \|\mathrm{cof}(\nabla \mathbf{F})\|_{L^\infty(Q),l} \left\| \frac{1}{w} \right\|^2_{L^\infty(Q)} \|w(u^h \circ \mathbf{F})\|^2_{L^2(Q)}$$

where $C_{inv} = C_{inv}(p_1, p_2, p_3)$ is the positive constant defined by (39), λ_Q is the local shape regularity constant of Q, and h_Q is the length of the largest side of Q. Finally, using Hölder's inequality again and then mapping back to physical space, we have

$$\|u^h\|^2_{L^2(\partial K)} \leq C_w C_{inv} \lambda_Q h_Q^{-1} \|\mathrm{cof}(\nabla \mathbf{F})\|_{L^\infty(Q),l} \|\det(\nabla \mathbf{F}^{-1})\|_{L^\infty(K),l} \|u^h\|^2_{L^2(K)}$$

where

$$C_w = \left\| \frac{1}{w} \right\|^2_{L^\infty(Q)} \|w\|^2_{L^\infty(Q)}.$$

The lemma follows by recalling the definitions of λ_K and h_K. □

We now present an extension of Lemma 4.4 to the general setting.

Theorem 4.2 *Let $K \in \mathcal{K}_h$ and $Q = \mathbf{F}^{-1}(K)$. Then, for all $u^h \in \mathcal{V}^h$,*

$$\|\nabla u^h \cdot \mathbf{n}\|^2_{L^2(\partial K)} \leq C_N C_{inv} \lambda_Q \lambda_K h_K^{-1} |u^h|^2_{H^1(K)} \tag{58}$$

where $C_{inv} = C_{inv}(p_1, p_2, p_3)$ is the positive constant defined by (39), λ_Q is the local shape regularity constant of Q, λ_K is the shape regularity constant defined by (32),

$$C_N = \left(C_1^{1/2} + C_2^{1/2}\right)^2, \tag{59}$$

$$C_1 = C_B \left\| \frac{1}{w} \right\|^2_{L^\infty(Q)} \left(\|w\|_{L^\infty(Q)} + \pi^{-1} C_{det} \|\nabla \mathbf{F}^{-1}\|_{L^\infty(K),l} \, |w|_{W^{1,\infty}(Q)} \, h_K \right)^2, \tag{60}$$

$$C_2 = \left(\pi^{-1} C_{det} \|\nabla \mathbf{F}^{-1}\|_{L^\infty(K),l} \left| \frac{1}{w} \right|_{W^{1,\infty}(Q)} \|w\|_{L^\infty(Q)} h_K \right)^2, \tag{61}$$

$$C_B = \left(1 + \sqrt{3} \|\nabla \mathbf{F}\|_{L^\infty(Q),l} \|\nabla^2 \mathbf{F}^{-1}\|_{L^\infty(K),l} h_K\right)^2, \tag{62}$$

and

$$C_{det} = \|\det(\nabla \mathbf{F})\|^{1/2}_{L^\infty(Q)} \|\det(\nabla \mathbf{F}^{-1})\|^{1/2}_{L^\infty(K)}. \tag{63}$$

Proof Let $u^h \in \mathcal{V}^h$. We employ a change of variables from physical space to parametric space to arrive at

$$\begin{aligned} \|\nabla u^h \cdot \mathbf{n}\|^2_{L^2(\partial K)} &\leq \int_{\partial K} |\nabla u^h|^2 \, d\mathbf{s} \\ &\leq \|\mathrm{cof}(\nabla \mathbf{F})\|_{L^\infty(Q),l} \int_{\partial Q} |\mathbf{D}^T \nabla \left(u^h \circ \mathbf{F}\right)|^2 \, d\mathbf{t} \\ &\leq \|\mathrm{cof}(\nabla \mathbf{F})\|_{L^\infty(Q),l} \int_{\partial Q} \left| \mathbf{D}^T \nabla \left(\frac{1}{w} w (u^h \circ \mathbf{F}) \right) \right|^2 d\mathbf{t} \end{aligned} \tag{64}$$

where we have denoted

$$\mathbf{D} = \nabla \mathbf{F}^{-1} \circ \mathbf{F}.$$

The product rule gives

$$\nabla \left(\frac{1}{w} w (u^h \circ \mathbf{F}) \right) = \frac{1}{w} \nabla \left(w (u^h \circ \mathbf{F}) \right) + w (u^h \circ \mathbf{F}) \nabla \left(\frac{1}{w} \right)$$

which in conjunction with (64) and the Cauchy–Schwarz inequality provides the expression

$$\|\nabla u^h \cdot \mathbf{n}\|^2_{L^2(\partial K)} \leq (A^{1/2} + B^{1/2})^2 \tag{65}$$

where

$$A = \|\mathrm{cof}(\nabla \mathbf{F})\|_{L^\infty(Q),l} \int_{\partial Q} \left| \frac{1}{w} \mathbf{D}^T \nabla (w(u^h \circ \mathbf{F})) \right|^2 d\mathbf{t}$$

and

$$B = \|\mathrm{cof}(\nabla \mathbf{F})\|_{L^\infty(Q),l} \int_{\partial Q} \left| w(u^h \circ \mathbf{F}) \mathbf{D}^T \nabla \left(\frac{1}{w} \right) \right|^2 d\mathbf{t}.$$

Invoking Hölder's inequality and the definition of the spectral norm for matrices, we can write

$$A \leq \|\mathrm{cof}(\nabla \mathbf{F})\|_{L^\infty(Q),l} \left\| \frac{1}{w} \right\|^2_{L^\infty(Q)} \int_{\partial Q} \left| \mathbf{D}^T \nabla (w(u^h \circ \mathbf{F})) \right|^2 d\mathbf{t} \tag{66}$$

and

$$B \leq \|\mathrm{cof}(\nabla \mathbf{F})\|_{L^\infty(Q),l} \left| \frac{1}{w} \right|^2_{W^{1,\infty}(Q)} \|\nabla \mathbf{F}^{-1}\|^2_{L^\infty(K),l} \|w(u^h \circ \mathbf{F})\|^2_{L^2(\partial Q)} \tag{67}$$

where we have taken advantage of our special definition for the $W^{1,\infty}$ semi-norm. We now proceed on separate paths to bound the A and B terms. We begin with the A term (66). Using an argument identical to the one appearing in the proof of Lemma 4.4, we obtain the bound

$$A \leq C_B C_{inv} \lambda_Q \lambda_K h_K^{-1} \left\| \frac{1}{w} \right\|^2_{L^\infty(Q)} |(w \circ \mathbf{F}^{-1}) u^h|^2_{H^1(K)}$$

where $C_{inv} = C_{inv}(p_1, p_2, p_3)$ is the positive constant defined by (39), λ_Q is the local shape regularity constant of Q, λ_K is the shape regularity constant defined by (32), and

$$C_B = \left(1 + \sqrt{3} \|\nabla \mathbf{F}\|_{L^\infty(Q),l} \|\nabla^2 \mathbf{F}^{-1}\|_{L^\infty(K),l} h_K \right)^2.$$

The product-rule, Cauchy–Schwarz, and Hölder's then give

$$A \leq C_B C_{inv} \lambda_Q \lambda_K h_K^{-1} \left\| \frac{1}{w} \right\|^2_{L^\infty(Q)} \left(A_1^{1/2} + A_2^{1/2} \right)^2 \tag{68}$$

where

$$A_1 = \|w\|^2_{L^\infty(Q)} |u^h|^2_{H^1(K)}$$

and

$$A_2 = |w|^2_{W^{1,\infty}(Q)} \|\nabla \mathbf{F}^{-1}\|^2_{L^\infty(K),l} \|u^h\|^2_{L^2(K)}.$$

We now proceed to bounding the B term. Recalling (67) and employing Lemma 4.2, we have

$$B \leq C_{inv} \lambda_Q h_Q^{-1} \|\text{cof}(\nabla \mathbf{F})\|_{L^\infty(Q),l} \left|\frac{1}{w}\right|^2_{W^{1,\infty}(Q)} \|\nabla \mathbf{F}^{-1}\|^2_{L^\infty(K),l} \|w(u^h \circ \mathbf{F})\|^2_{L^2(Q)}.$$

Invoking Hölder's inequality, we further write

$$B \leq C_{inv} \lambda_Q h_Q^{-1} \|\text{cof}(\nabla \mathbf{F})\|_{L^\infty(Q),l} \left|\frac{1}{w}\right|^2_{W^{1,\infty}(Q)} \|w\|^2_{L^\infty(Q)} \|\nabla \mathbf{F}^{-1}\|^2_{L^\infty(K),l} \|u^h \circ \mathbf{F}\|^2_{L^2(Q)}.$$

We finally map back to physical space, obtaining the expression

$$B \leq C_{inv} \lambda_Q \lambda_K h_K^{-1} \left|\frac{1}{w}\right|^2_{W^{1,\infty}(Q)} \|w\|^2_{L^\infty(Q)} \|\nabla \mathbf{F}^{-1}\|^2_{L^\infty(K),l} \|u^h\|^2_{L^2(K)}. \tag{69}$$

Collecting Eqs. (65), (68), and (69) and rearranging terms, we have

$$\|\nabla u^h \cdot \mathbf{n}\|^2_{L^2(\partial K)} \leq C_{inv} \lambda_Q \lambda_K h_K^{-1} (\tilde{A}^{1/2} + \tilde{B}^{1/2})^2 \tag{70}$$

where

$$\tilde{A} = C_B \left\|\frac{1}{w}\right\|^2_{L^\infty(Q)} \left(\|w\|_{L^\infty(Q)} |u^h|_{H^1(K)} + |w|_{W^{1,\infty}(Q)} \|\nabla \mathbf{F}^{-1}\|_{L^\infty(K),l} \|u^h\|_{L^2(K)}\right)^2$$

and

$$\tilde{B} = \left(\left|\frac{1}{w}\right|_{W^{1,\infty}(Q)} \|w\|_{L^\infty(Q)} \|\nabla \mathbf{F}^{-1}\|_{L^\infty(K),l} \|u^h\|_{L^2(K)}\right)^2.$$

Our objective is to bound the $\|u^h\|_{L^2(K)}$ terms in $\tilde{A}$ and $\tilde{B}$ with terms proportional to $|u^h|_{H^1(K)}$. We recognize that

$$\|\nabla u^h \cdot \mathbf{n}\|^2_{L^2(\partial K)} = \|\nabla (u^h - z^h) \cdot \mathbf{n}\|^2_{L^2(\partial K)} \tag{71}$$

for all constant $z^h \in \mathcal{V}^h$. Let us choose z^h to be equal to

$$z^h = \frac{1}{|Q|} \int_Q (u^h \circ \mathbf{F})\, d\boldsymbol{\xi}$$

where $|Q|$ is the volume of the parallelepiped Q. Using change of variables and Hölder's inequality, we have

$$\|u^h - z^h\|_{L^2(K)} \leq \|\det(\nabla \mathbf{F})\|^{1/2}_{L^\infty(Q)} \|u^h \circ \mathbf{F} - z^h\|_{L^2(Q)}.$$

Since z^h is equal to the average of $u^h \circ \mathbf{F}$ over Q, we can employ Poincaré's inequality for a rectangular parallelepiped domain [9] to further write

$$\|u^h - z^h\|_{L^2(K)} \leq \pi^{-1} h_Q \|\det(\nabla \mathbf{F})\|^{1/2}_{L^\infty(Q)} |u^h \circ \mathbf{F}|_{H^1(Q)}.$$

Finally, we map back to K:

$$\|u^h - z^h\|_{L^2(K)} \leq \pi^{-1} h_K \|\det(\nabla \mathbf{F})\|^{1/2}_{L^\infty(Q)} \|\det(\nabla \mathbf{F}^{-1})\|^{1/2}_{L^\infty(K)} |u^h|_{H^1(K)}. \quad (72)$$

By replacing u^h with $u^h - z^h$ in (70) and applying inequality (72), we obtain the desired final expression. □

Note that if we take the physical mesh size $h_K \to 0$ and keep the parametric mapping $\mathbf{F}$ fixed, the constant C_N appearing in the above theorem will tend to $\left\| \frac{1}{w} \right\|^2_{L^\infty(Q)} \|w\|^2_{L^\infty(Q)}$. Hence, we recover a similar inequality to that appearing in Theorem 4.1 with mesh refinement. This suggests that we may be able to ignore in practice higher-order terms due to the nonlinear geometrical mapping. Moreover, if the NURBS weighting function is chosen such that it is locally constant, we recover the inequality appearing in Lemma 4.4. Finally, by employing a similar method of proof to that of Theorem 4.2, we can obtain discrete trace inequalities for higher-order boundary derivatives. For example, we can show that for a given element $K \in \mathcal{K}_h$ with $Q = \mathbf{F}^{-1}(K)$,

$$\|\Delta u^h\|^2_{L^2(\partial K)} \leq C_N C_{inv} \lambda_Q \lambda_K h_K^{-1} \|u^h\|^2_{H^2(K)}$$

for every $u^h \in \mathcal{V}^h$ where

$$C_N = \left\| \frac{1}{w} \right\|^2_{L^\infty(Q)} \|w\|^2_{L^\infty(Q)} + O(h_K).$$

5 Application to a Laplace problem

In this section, we discuss the application of our explicit trace inequalities in the numerical solution of a simple Laplace problem driven by Dirichlet boundary conditions: given $g : \partial\Omega \to \mathbb{R}$, find $u : \Omega \to \mathbb{R}$ such that

$$-\Delta u = 0 \quad \text{in } \Omega \quad (73)$$

$$u = g \quad \text{on } \partial\Omega. \quad (74)$$

As was discussed in the introduction, strong imposition of Dirichlet boundary conditions is cumbersome and non-intuitive in NURBS-based isogeometric analysis. Unlike Lagrange finite elements, NURBS basis functions do not interpolate function values at nodal points. Strong imposition of Dirichlet boundary conditions is made even more difficult to implement in the context of complex, three-dimensional geometries. For this reason, we choose to instead utilize Nitsche's method [29] as a means of weakly enforcing the Dirichlet boundary conditions appearing in our boundary value problem. The corresponding discrete problem is as follows: find $u^h \in \mathcal{V}^h$ such that

$$b^h(u^h, v^h) = l^h(v^h), \quad \forall v^h \in \mathcal{V}^h \tag{75}$$

where

$$\begin{aligned} b^h(u^h, v^h) = &\int_\Omega \nabla u^h \cdot \nabla v^h \, d\mathbf{x} - \int_{\partial\Omega} (\nabla u^h \cdot \mathbf{n}) v^h \, d\mathbf{s} - \int_{\partial\Omega} (\nabla v^h \cdot \mathbf{n}) u^h \, d\mathbf{s} \\ &+ \sum_K C_K \int_{\partial K} u^h v^h I_{\partial\Omega} \, d\mathbf{s} \end{aligned} \tag{76}$$

and

$$l^h(v^h) = -\int_{\partial\Omega} (\nabla v^h \cdot \mathbf{n}) g \, d\mathbf{s} + \sum_K C_K \int_{\partial K} g v^h I_{\partial\Omega} \, d\mathbf{s} \tag{77}$$

in which $\mathbf{n}$ denotes the outward pointing normal to $\partial\Omega$, C_K denotes an element-wise tunable parameter, and

$$I_{\partial\Omega}(s) = \begin{cases} 1 & \text{if } s \in \partial\Omega \\ 0 & \text{otherwise.} \end{cases} \tag{78}$$

It is easily shown that the discrete formulation given by (75) is consistent. The following lemma provides sufficient lower bounds for C_K in order to ensure ellipticity.

Lemma 5.1 *Suppose that, for every element $K \in \mathcal{K}_h$,*

$$C_K \geq 4 C_N C_{inv} \lambda_Q \lambda_K h_K^{-1} \tag{79}$$

where $C_{inv} = C_{inv}(p_1, p_2, p_3)$ is the positive constant defined by (39), λ_Q is the local shape regularity constant of Q, λ_K is the shape regularity constant defined by (32), and C_N is the positive constant defined by (59). Then

$$b^h(v^h, v^h) \geq \frac{1}{2} \|v^h\|_E^2 \tag{80}$$

where

$$\|v^h\|_E = \left(|v^h|^2_{H^1(K)} + \sum_K C_K \int_{\partial K} |v^h|^2 I_{\partial\Omega}\, ds \right)^{1/2}. \tag{81}$$

Proof Let $v^h \in \mathcal{V}^h$. By definition, we have

$$b^h(v^h, v^h) = \int_\Omega |\nabla v^h|^2\, d\mathbf{x} - 2\int_{\partial\Omega} (\nabla v^h \cdot \mathbf{n}) v^h\, d\mathbf{s} + \sum_K C_K \int_{\partial K} |v^h|^2 I_{\partial\Omega}\, d\mathbf{s}. \tag{82}$$

An application of Young's inequality yields

$$\int_{\partial\Omega} (\nabla v^h \cdot \mathbf{n}) v^h\, d\mathbf{s} \leq \sum_K \frac{1}{C_K} \int_{\partial K} |\nabla v^h \cdot \mathbf{n}|^2 I_{\partial\Omega}\, d\mathbf{s} + \sum_K \frac{C_K}{4} \int_{\partial K} |v^h|^2 I_{\partial\Omega}\, d\mathbf{s}. \tag{83}$$

By Theorem 4.2 and (79), we can write

$$\int_{\partial\Omega} (\nabla v^h \cdot \mathbf{n}) v^h\, d\mathbf{s} \leq \frac{1}{4} |v^h|^2_{H^1(K)} + \sum_K \frac{C_K}{4} \int_{\partial K} |v^h|^2 I_{\partial\Omega}\, d\mathbf{s}. \tag{84}$$

Collecting all of our inequalities, we arrive at the desired estimate. □

Under reasonable regularity assumptions, it is a simple exercise to show that the discrete solution of the Laplace problem converges to the exact solution when C_K scales inversely with the local mesh size and the hypothesis of the above lemma is satisfied. Furthermore, optimal error estimates in both the H^1-norm and the L^2-norm can be derived. To verify these estimates, we have numerically solved a Laplace problem subject to Dirichlet boundary conditions on a three-dimensional quarter annulus. The inner radius of the quarter annulus is taken to be one and the outer radius and height of the quarter annulus are taken to be two. The exact solution, taken to be $u = \sin(x)\exp(y)$, is visualized in Fig. 1. In accordance with Lemma 5.1, we utilized a penalty parameter of

$$C_K = 4 C_N C_{inv} \lambda_Q \lambda_K h_K^{-1}$$

in our numerical simulations. We ignored the higher-order terms appearing in C_N in calculating the penalty parameter C_K, and we approximated all max-norm quantities by sampling at Gauss quadrature points. As is standard in isogeometric analysis, we employed $p+1$ quadrature points per element in each parametric direction. In Fig. 2a and b, we have plotted the H^1 error and L^2 error versus the mesh size for C^{p-1}-continuous NURBS discretizations of uniform degree $p = 2, 3, 4$. From the given plots, it is apparent that the discrete solution optimally converges to the exact solution in both the H^1-norm and the L^2-norm.

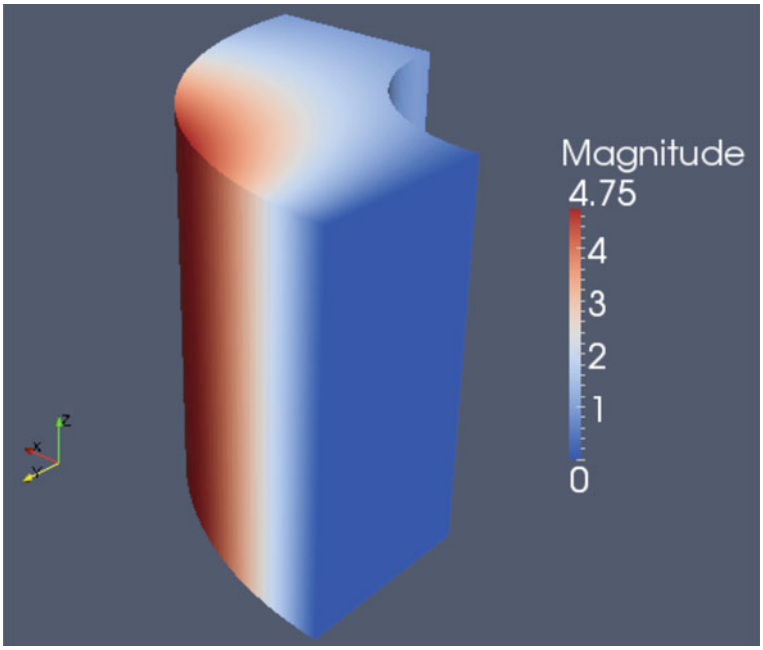

Fig. 1 Exact solution of the Laplace problem on a three-dimensional quarter annulus

6 Patch-wise trace inequalities

The trace inequalities that have been discussed so far in this paper have been element-wise in nature. It is an immediate corollary of these inequalities that analogous trace inequalities exist at the global patch-wise level, with possibly smaller trace constants. In what follows, we consider discrete trace inequalities of the form:

$$\|u^h\|^2_{L^2(\partial\Omega)} \leq C_{patch}\|u^h\|^2_{L^2(\Omega)}. \tag{85}$$

We further restrict ourselves to the two-dimensional setting, setting $\Omega = (0,1)^2$. In Table 3, we have, for uniform C^{p-1}-continuous B-spline discretizations, listed optimal values for the bounding constant in (85) normalized by the global mesh size h. Note that for polynomial degrees $p > 0$, the optimal normalized bounding constant decreases in magnitude as the patch increases in size. Furthermore, for the higher-refined meshes, it appears that the optimal normalized bounding constant linearly scales with p in contrast with the standard quadratic scaling. To better see this trend, we have graphically depicted the normalized optimal bounding constants in Fig. 3. From this plot, it is evident that for a given patch size, the optimal bounding constant pre-asymptotically scales like p and asymptotically scales like p^2. The theoretical tools employed in this paper are unable to explain this pre-asymptotic behavior, and we surmise that any successful analytical investigation will likely require a B-spline analogue of orthogonal polynomials. Such an investigation is beyond the scope of the

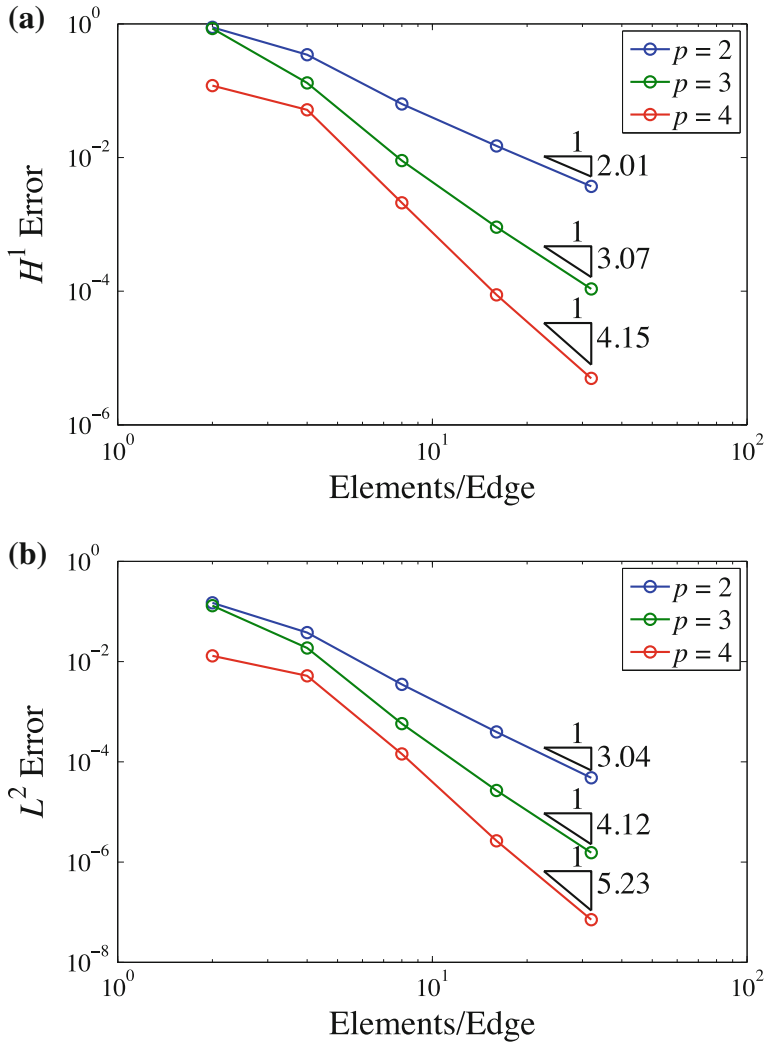

Fig. 2 Error of the discrete solution of the Laplace problem: **a** H^1 error, **b** L^2 error

current paper. We have found that the enhanced pre-asymptotic behavior exhibited by B-spline discretizations of maximal continuity is not shared for low-continuity discretizations.

7 Conclusions

In this paper, we have derived new trace inequalities for use in NURBS-based isogeometric analysis. All dependencies on shape, size, polynomial degree, and the NURBS weighting function are precisely specified in our analysis, and explicit values are

Table 3 Optimal values for the bounding constant in (85) normalized by the global mesh size h

Polynomial degree	1×1 Mesh	2×2 Mesh	4×4 Mesh	8×8 Mesh	16×16 Mesh
0	6	6	6	6	6
1	12	8	7	6.93...	6.93...
2	24	16	13.71...	13.36...	13.35...
3	40	26	21.74...	20.92...	20.86...
4	60	38	30.91...	29.40...	29.24...
5	84	52	41.14...	38.64...	38.32...
6	112	68	52.40...	48.55...	48.01...
7	144	86	64.68...	59.08...	58.23...
8	180	106	77.98...	70.19...	68.93...
9	220	128	92.28...	81.86...	80.05...
10	264	152	107.59...	94.07...	91.56...

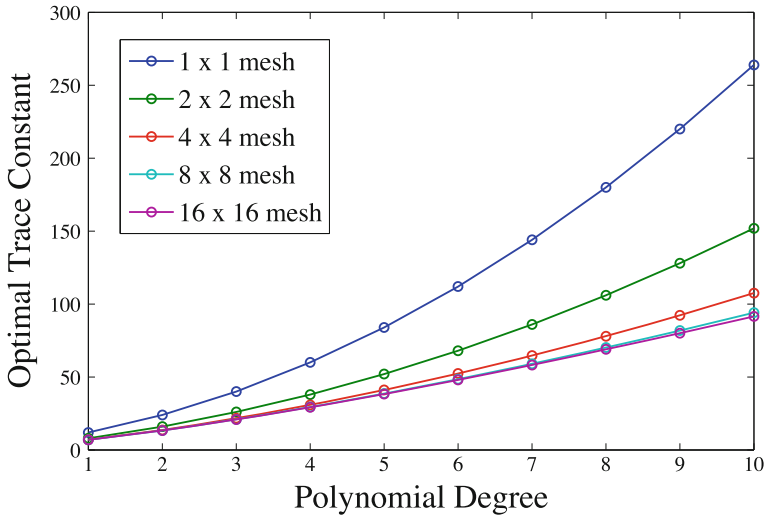

Fig. 3 Optimal values for the bounding constant in (85) normalized by the global mesh size h

provided for all bounding constants appearing in our estimates. Consequently, these inequalities can be directly utilized in the design of stabilization parameters appearing in Nitsche's method, an attractive candidate for the weak enforcement of strong boundary conditions in isogeometric analysis. As hexahedral finite elements are special cases of NURBS, our results specialize to parametric hexahedral finite elements. Moreover, as our results are local in the sense that they apply element-wise, our analysis generalizes to T-spline-based isogeometric analysis. We compared the bounding constants appearing in our explicit inequalities with numerically computed optimal bounding constants and found that our explicit bounding constants scale optimally with both polynomial degree and shape regularity. We finished this paper with a numerical

investigation of trace inequalities on the patch level which revealed that patch-wise optimal trace constants pre-asymptotically scale like p in contrast with the standard quadratic scaling provided that B-spline discretizations of maximal continuity are employed. A theoretical exploration of this phenomena is underway.

Acknowledgments J.A. Evans and T.J.R. Hughes were partially supported by the Office of Naval Research under Contract No. N00014-08-0992. This support is gratefully acknowledged.

8 Appendix A: An alternate Hölder inequality

Lemma A.1 *Let $D \subset \mathbb{R}^d$ denote an open domain for d a positive integer. If $f \in L^\infty(D)$ and $g \in L^2(D)$, then*

$$\|fg\|_{L^2(D)} \leq \|f\|_{L^\infty(D)} \|g\|_{L^2(D)}. \tag{86}$$

Proof Let $f \in L^\infty(D)$ and $g \in L^2(D)$. By construction,

$$\|fg\|_{L^2(D)} = \|f^2 g^2\|_{L^1(D)}^{1/2}.$$

By the classical Hölder Inequality,

$$\begin{aligned} \|fg\|_{L^2(D)} &\leq (\|f^2\|_{L^\infty(D)} \|g^2\|_{L^1(D)})^{1/2} \\ &= (\|f\|_{L^\infty(D)}^2 \|g\|_{L^2(D)}^2)^{1/2} \\ &= \|f\|_{L^\infty(D)} \|g\|_{L^2(D)}. \end{aligned} \tag{87}$$

□

References

1. Adams, R.A.: Sobolev Spaces. Academic Press, London (1975)
2. Arnold, D.: An interior penalty finite element method with discontinuous elements. SIAM J. Numer. Anal. **19**, 742–760 (1982)
3. Arrieta, J.M., Rodríguez-Bernal, A., Rossi, J.D.: The best Sobolev trace constant as limit of the usual Sobolev constant for small strips near the boundary. Proc. R. Soc. Edinb. Sect. A Math. **138**, 223–237 (2008)
4. Bazilevs, Y., Calo, V.M., Cottrell, J.A., Evans, J.A., Hughes, T.J.R., Lipton, S., Scott, M.A., Sederberg, T.W.: Isogeometric analysis using T-splines. Comput. Methods Appl. Mech. Eng. **199**, 229–263 (2010)
5. Bazilevs, Y., Calo, V.M., Hughes, T.J.R., Zhang, Y.: Isogeometric fluid-structure interaction: Theory, algorithms, and computations. Comput. Mech. **43**, 3–37 (2008)
6. Bazilevs, Y., da Veiga, L., Cottrell, J.A., Hughes, T.J.R., Sangalli, G.: Isogeometric analysis: Approximation, stability and error estimates for h-refined meshes. Math. Models Methods Appl. Sci. **16**, 1–60 (2006)
7. Bazilevs, Y., Michler, C.M., Calo, V.M., Hughes, T.J.R.: Weak Dirichlet boundary conditions for wall-bounded turbulent flows. Comput. Methods Appl. Mech. Eng. **196**, 4853–4862 (2007)
8. Bazilevs, Y., Michler, C.M., Calo, V.M., Hughes, T.J.R.: Isogeometric variational multiscale modeling of wall-bounded turbulent flows with weakly-enforced boundary conditions on unstretched meshes. Comput. Methods Appl. Mech. Eng. **199**, 780–790 (2010)

9. Bebendorf, M.: A note on the Poincaré inequality for convex domains. Zeitschrift für Analysis und ihre Anwendungen **22**, 751–756 (2003)
10. Beckner, W.: Sharp Sobolev inequalities on the sphere and the Moser-Trudinger inequality. Ann. Math. **138**, 213–242 (1993)
11. Beirão da Veiga, L., Buffa, A., Rivas, J., Sangalli, G.: Some estimates for $h - p - k$ refinement in isogeometric analysis. Numerische Mathematik **118**, 271–305 (2011)
12. Buffa, A., Sangalli, G., Vázquez, R.: Isogeometric analysis in electromagnetics: B-splines approximation. Comput. Methods Appl. Mech. Eng. **199**, 1143–1152 (2010)
13. Burkhart, D., Hamann, B., Umlauf, G.: Iso-geometric analysis based on Catmull-Clark subdivision solids. Comput. Graph. Forum **29**, 1575–1584 (2010)
14. Cottrell, J.A., Hughes, T.J.R., Bazilevs, Y.: Isogeometric analysis: Toward integration of CAD and FEA. Wiley, New York (2009)
15. Cottrell, J.A., Reali, A., Bazilevs, Y., Hughes, T.J.R.: Isogeometric analysis of structural vibrations. Comput. Methods Appl. Mech. Eng. **195**, 5257–5296 (2006)
16. Dorfel, M.R., Jüttler, B., Simeon, B.: Adaptive isogeometric analysis by local h-refinement using T-splines. Comput. Methods Appl. Mech. Eng. **199**, 264–275 (2010)
17. Elguedj, T., Bazilevs, Y., Calo, V.M., Hughes, T.J.R.: B-bar and F-bar projection methods for nearly incompressible linear and nonlinear elasticity and plasticity using higher-order NURBS elements. Comput. Methods Appl. Mech. Eng. **197**, 2732–2762 (2008)
18. Embar, A., Dolbow, J., Harari, I.: Imposing Dirichlet boundary conditions with Nitsche's method and spline-based finite elements. Int. J. Numer. Methods Eng. **83**, 877–898 (2010)
19. Epschteyn, Y., Rivière, B.: Estimation of penalty parameters for symmetric interior penalty Galerkin methods. J. Comput. Appl. Math. **206**, 843–872 (2007)
20. Escobar, J.F.: Sharp constant in a Sobolev trace inequality. Indiana Univ. Math. J. **37**, 687–698 (1988)
21. Evans, J.A., Bazilevs, Y., Babuška, I., Hughes, T.J.R.: n-widths, sup-infs, and optimality ratios for the k-version of the isogeometric finite element method. Comput. Methods Appl. Mech. Eng. **198**, 1726–1741 (2009)
22. Gomez, H., Calo, V.M., Bazilevs, Y., Hughes, T.J.R.: Isogeometric analysis of the Cahn–Hilliard phase-field model. Comput. Methods Appl. Mech. Eng. **197**, 4333–4352 (2008)
23. Harari, I., Hughes, T.J.R.: What are C and h? Inequalities for the analysis and design of finite element methods. Comput. Methods Appl. Mech. Eng. **97**, 157–192 (1992)
24. Hughes, T.J.R., Cottrell, J.A., Bazilevs, Y.: Isogeometric analysis: CAD, finite elements, NURBS, exact geometry, and mesh refinement. Comput. Methods Appl. Mech. Eng. **194**, 4135–4195 (2005)
25. Kiendl, J., Bletzinger, K.-U., Linhard, J., Wüchner, R.: Isogeometric shell analysis with Kirchhoff–Love elements. Comput. Methods Appl. Mech. Eng. **198**, 3902–3914 (2009)
26. Lang, S.: Fundamentals of Differential Geometry. Springer-Verlag, Berlin (1999)
27. Lions, P.-L.: The concentration-compactness principle in the calculus of variations. The locally compact case II. Revista Matemática. Iberoamericana **1**, 45–121 (1985)
28. Lipton, S., Evans, J.A., Bazilevs, Y., Elguedj, T., Hughes, T.J.R.: Robustness of isogeometric structural discretizations under severe mesh distortion. Comput. Methods Appl. Mech. Eng. **199**, 357–373 (2010)
29. Nitsche, J.A.: Über ein Variationspringzip zur Lösung von Dirichlet-Problemem bei Verwendung von Teilräumen, die keinen Randbedingungen unterworfen sind. Abhandlungen aus dem Mathematischen Seminar der Universit at Hamburg **36**, 9–15 (1971)
30. Piegl, L., Tiller, W.: The NURBS Book. Springer-Verlag, Berlin (1997)
31. Shahbazi, K.: An explicit expression for the penalty parameter of the interior penalty method. J. Comput. Phys. **205**, 401–407 (2005)
32. Vesser, A., Verfürth, R.: Explicit upper bounds for dual norms of residuals. SIAM J. Numer. Anal. **47**, 2387–2405 (2009)
33. Warburton, T., Hesthaven, J.S.: On the constants in hp-finite element trace inverse inequalities. Comput. Methods Appl. Mech. Eng. **192**, 2765–2773 (2003)
34. Wheeler, M.F.: An elliptic collocation-finite element method with -interior penalties. SIAM J. Numer. Anal. **15**, 152–161 (1978)